



A cross-scale hygro-mechanical coupling model for hollow glass bead/resin composite materials

Jingze Wang, Weicheng Cui*

Key Laboratory of Coastal Environment and Resources of Zhejiang Province, School of Engineering, Westlake University, 600 Duny Road, Hangzhou 310030, Zhejiang Province, China

ARTICLE INFO

Keywords:

Hollow glass bead
Composite
Cross-scale
Couple
Hygroscopic

ABSTRACT

Hollow glass bead/resin composite materials are now mainly used in the deep sea submersibles. They are also targeted for application in aviation, aerospace and military applications in the future because of their good material properties, such as low density and high compressive strength. However, there is a coupling relationship between the stress and hygroscopicity in their water absorption process. This reduce the safety of structures produced by hollow glass bead/resin composite materials, especially the underwater and deep-sea structures. In this paper, a hygro-mechanical coupling model and its simplified model for hollow glass bead/resin composites are proposed based on Fick's second law. A number of experiments are conducted to validate these two models. Comparisons of the predictions of these two models with experimental data show good agreement. The distribution and variation of the stress, water absorption and diffusion coefficient of the composite during the water absorption process were studied. The relationship between the deviation and the water absorption in the simplified model has been given. These results can guide the engineering application of hollow glass bead/resin composite materials, especially in deep sea environments.

1. Introduction

The water absorption has a negative impact on the safety of composite structures, especially the underwater and deep-sea structures (Ishai, 1975; Zhong and Zhou, 1999; Selzer and Friedrich, 1997; Obeid et al., 2018). At present, hollow glass bead/resin composite materials are mainly used in deep-sea fields to provide buoyancy for manned/unmanned submersibles (Hou et al., 2020; Le Gall et al., 2014). Additionally they also have good prospects in aviation, aerospace and military applications based on their low weight and high compressive strength. For example, they can be combined with fibre-reinforced composites to form a sandwich structure for wings or spacecraft shells (Corigliano et al., 2000). They can even be used as functional composites in marine, electronics, aerospace and military/defence requisitions. (Ren et al., 2017; Niu et al., 2022). However, the uncertainty of safety after water absorption hinders the application of hollow glass bead/resin composite materials.

At present, scholars generally agree that the water absorption behaviour of polymer-based composites follows Fick's second law and that the water absorption is linear with the square root of time (Shen and Springer, 1976; Kumosa et al., 2004; Boukert et al., 2019; Peret et al.,

2019; Lee and Peppas, 1993). However, a large number of experiments on water absorption in composites have shown that the ratio of water absorption to the square root of time decreases significantly after a linear phase and that water absorption is no longer linear with the square root of time (Gueribiz et al., 2013; Meng et al., 2016). Carter (1978) and Roy et al. (2000) suggested that this nonlinear segment is caused by the variation in the diffusion coefficient and developed the Langmuir model and the diffusion coefficient variation model, respectively. Neuman et al. (1985) argued that there is a coupling relationship between the internal stress and the water absorption in the polymer matrix based on the free volume theory. This coupling relationship changes the diffusion coefficient and causes a nonlinear stage in the water absorption process of composites. The functional relationship between the diffusion coefficient and stress is:

$$D_{\sigma} = D_0 \exp\left(\frac{\alpha\sigma}{G_m}\right) \quad (1)$$

where, σ is the stress to which the matrix is subjected, and when the matrix is subjected to three-way stress, σ is the bulk stress. α is a coefficient, $\alpha = 6 \sim 10$. Peret et al. (2017) analyzed the impacts of

* Corresponding author.

E-mail address: cuiweicheng@westlake.edu.cn (W. Cui).

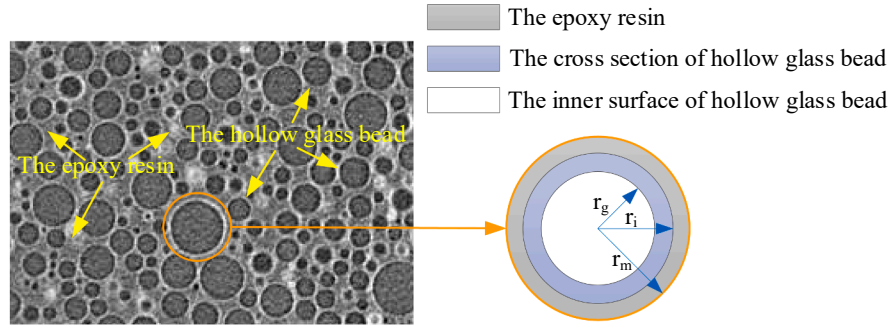


Fig. 1. The representative volume element (RVE) at micro scale for the hollow glass bead/resin composite materials.

mechanical loading on the diffusion coefficient by implementing the free volume theory in a FE software. Shen et al. (1976) proposed a composite water absorption model as follows:

$$\frac{C(z)}{C_m} = 1 - \frac{4}{\pi} \sum_{j=1}^{\infty} \frac{1}{(2j+1)} \sin \frac{(2j+1)\pi z}{h} \exp \left[-\frac{(2j+1)^2 \pi^2 D t}{h^2} \right] \quad (2)$$

where, $C(z)$ is the water absorption at z . D is the diffusion coefficient of the composite. The diffusion coefficient of the composite laminate can be calculated as follows (Shen et al., 1976):

$$D = \pi \left(\frac{h}{4C_m} \right)^2 \left(\frac{C_2 - C_1}{\sqrt{t_2} - \sqrt{t_1}} \right)^2 \quad (3)$$

where, C_1 and C_2 are the water absorptions corresponding to t_1 and t_2 , respectively.

The reported study of hygro-mechanical coupling in the water absorption process of composites is mostly focused on fibre-reinforced composites. Gueribiz and Jacquemin (2013) simulated the diffusion behaviour of water molecules in fibre-reinforced composites based on a representative volume element (RVE) model and calculated the water distribution. The existence of hygro-mechanical coupling in the water absorption process of fibre-reinforced composites was confirmed. Wang et al. (2017) proposed a multiscale coupled theoretical model of water absorption in fibre-reinforced composites. An equivalent diffusion time model is also proposed to calculate the water absorption when the diffusion coefficient changes with time:

$$T_n = \frac{T_{n-1} D_{n-1}}{D_n} + \Delta t_n \quad (4)$$

where Δt is the n th time period in the moisture absorption process after discretization; T_{n-1} and T_n are the equivalent diffusion times after the $(n-1)$ th and n th equivalents, respectively; and D_{n-1} and D_n are the diffusion coefficients corresponding to T_{n-1} and T_n , respectively. The theoretical prediction results were in good agreement with the experimental results. On this basis, a simplified model was further developed to be applicable to the engineering field (Wang et al., 2012):

$$D_\sigma = D_0 \exp \left\{ \frac{2\alpha(1 + \mu_m)}{1 - 2\mu_m} [kM^c + a\sigma_{11}^c + b(\sigma_{22}^c + \sigma_{33}^c)] \right\} \quad (5)$$

where, α is a constant with a range of 6 to 10. k , a and b are constants related to the properties of composite laminates. M^c is the water absorption of composite laminates, and σ_{11}^c , σ_{22}^c and σ_{33}^c are stresses on composite plies in the 1, 2, and 3 directions, respectively.

Water absorption of hollow glass bead/resin composites directly increases the material density and then has a negative effect on its service performance. In addition, water absorption by polymers causes plasticization and hydrolysis, triggering crack expansion and reducing strength (Selzer and Friedrich, 1997; Apicella and Nicolais, 1985; Guo et al. 2021; David et al., 1993; Ghorbed and valentin, 1993). Therefore, the water absorption of hollow glass bead/resin composites is extremely harmful to the safety and performance of deep-sea manned/unmanned

submersibles. Besides this, the uncertainty of safety caused by water absorption hinders the application of hollow glass bead/resin composites in other fields. In this paper, some experiments have been conducted to prove that hollow glass bead/resin composites also have the coupling behavior of stress and water absorption. A new hygro-mechanical coupling model is proposed. The distribution and variation of the stress, water absorption and diffusion coefficient and the effects of several material parameters on the water absorption behaviour are investigated. A simplified model is also developed for quick design calculations.

2. Theoretical derivation

2.1. Basic assumptions

The internal stress in the hollow glass bead/resin composites are mainly caused by the water absorption of the matrix. Therefore, the stress in the matrix should be calculated first, including those at both micro and meso scales. There are some methods calculating the internal stress of fiber reinforced composites (Catalanotti and Sebaey, 2019; Wang et al., 2022). However, only a few studies are carried out on the calculation of the internal stress of hollow glass bead composites.

The spatial distribution of hollow glass beads within the hollow glass bead/resin composite as well as the particle size are random (see Fig. 1), which causes difficulties in the establishment of the theoretical model.

Based on the assumption that the vacuum is constant for all hollow glass beads, the concentric spherical shell structure (see Fig. 1) is selected as an RVE. In reference (Wang and Cui, 2020), a concentric spherical shell model for hollow glass bead/resin composites by self-consistent theory was proposed. However, it focused on the stress distribution in hollow glass beads and did not consider the effect of hygroscopic rate. Therefore, the effect of hygroscopic rate needs to be further investigated. The basic assumptions are as follows:

- 1) Both glass and epoxy resins are isotropic materials, and hollow glass bead/resin composites are also considered to be isotropic at the mesoscale.
- 2) The vacuum of hollow glass beads is constant.
- 3) The RVE of hollow glass beads with average particle size can represent the properties of hollow glass bead/resin composites.

2.2. Calculation of bulk stress at the microscale

The concentric spherical shell model consists of a hollow glass spherical shell and an epoxy resin spherical shell. Without considering the water pressure, the pressure on the inner and outer surfaces is zero. The radial stress exists at the interface of the two spherical shells. Since the size of the RVE is at the micron level, we call the stress at this scale micro stress. According to the theory of elastic mechanics, the radial and tangential stress distributions in glass beads and epoxy resin are:

$$\left\{ \begin{array}{l} \sigma_{r_g} = -\frac{1 - \frac{r_g^3}{r_i^3}}{\frac{r_g^3}{r_i^3} - 1} \sigma_{r_i} \\ \sigma_{T_g} = -\frac{1 + \frac{r_g^3}{2r_i^3}}{\frac{r_g^3}{r_i^3} - 1} \sigma_{r_i} \end{array} \right. \quad (r_g \leq r \leq r_i) \text{ and } \left\{ \begin{array}{l} \sigma_{r_m} = -\frac{\frac{r_m^3}{r_i^3} - 1}{\frac{r_m^3}{r_i^3} - 1} \sigma_{r_i} \\ \sigma_{T_m} = \frac{\frac{r_m^3}{2r_i^3} + 1}{\frac{r_m^3}{r_i^3} - 1} \sigma_{r_i} \end{array} \right. \quad (r_i \leq r \leq r_m) \quad (6)$$

where, r_g , r_i and r_m are shown in Fig. 1. r is a variable. Both the stress equilibrium and displacement coordination conditions occur at the interface, and substituting $r = r_i$ into Eq. (6) yields:

$$\sigma_{r_g} = \sigma_{r_m} = -\sigma_{r_i} \quad (7)$$

This means that the stress equilibrium condition at the interface is automatically satisfied. The coupling behaviour of water absorption and stress is caused by the bulk stress of the resin. The bulk stress of the epoxy resin is obtained according to the theory of elastic mechanics as follows (Sadd, 2009):

$$\Theta^{mic} = \sigma_{r_m} + 2\sigma_{T_m} = \frac{3r_i^3}{r_m^3 - r_i^3} \sigma_{r_i} \quad (8)$$

In this equation, there is only one unknown parameter σ_{r_i} . Once this parameter is known, the bulk stress of the resin can be obtained, and then the relationship between the diffusion coefficient of the hollow glass bead/resin composite and the stress can be calculated. To simplify the calculation process, two parameters are defined:

$$\left\{ \begin{array}{l} G_p = \frac{2 + V_h}{2(1 - V_h)} \\ M_p = \frac{1 + 2V_g}{2(1 - V_g)} \end{array} \right. \quad (9)$$

where, V_h is the hollowness of hollow glass beads, $V_h = r_g^3/r_i^3$. V_g is the volume fraction of the hollow glass bead/resin composite accounted for by the glass beads (including the hollow part), $V_g = r_i^3/r_m^3$. Substituting $r = r_i$ into Eq. (6) yields the tangential stress at the interface:

$$\left\{ \begin{array}{l} \sigma_{T_g} = -\frac{1 + \frac{r_g^3}{2r_i^3}}{\frac{r_g^3}{r_i^3} - 1} \sigma_{r_i} \\ \sigma_{T_m} = \frac{\frac{r_m^3}{2r_i^3} + 1}{\frac{r_m^3}{r_i^3} - 1} \sigma_{r_i} \end{array} \right. \Rightarrow \left\{ \begin{array}{l} \sigma_{T_g} = G_p \sigma_{r_i} \\ \sigma_{T_m} = M_p \sigma_{r_i} \end{array} \right. \quad (10)$$

Hollow glass beads and epoxy resin are isotropic materials. The resin expands after absorbing water and is bound by the glass beads; then,

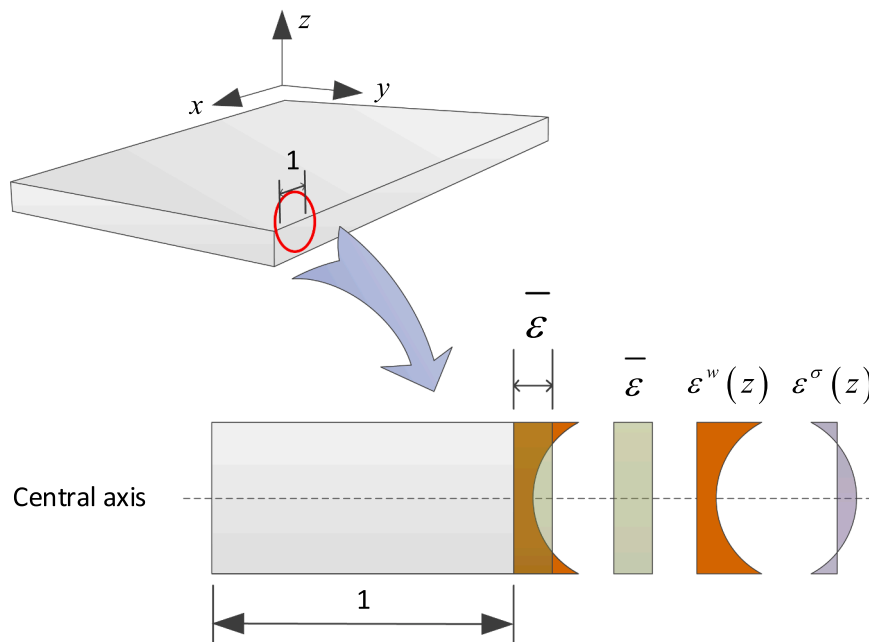


Fig. 2. Strains at meso scale for the hollow glass bead/resin composite materials after water absorption.

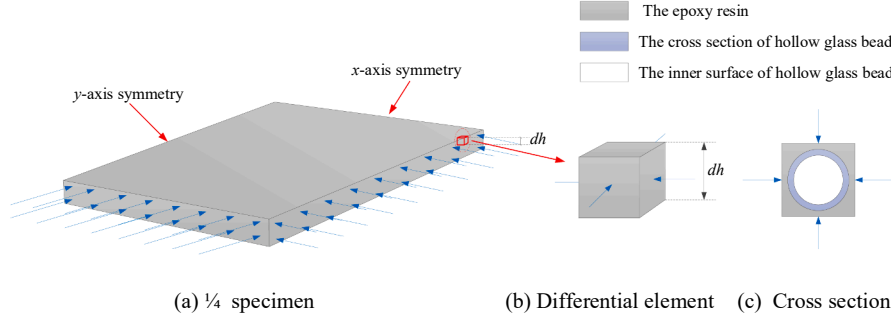


Fig. 3. The spherical shell-cubic model and its load case after water absorption.

internal stresses occur. The strain of glass beads is generated by stress only, while the strain of resin is generated by stress and water absorption. Therefore, the tangential strain of hollow glass beads as well as epoxy resin at the interface is:

$$\begin{cases} \varepsilon_{Tg} = \frac{1}{E_g} [(1 - \mu_g)\sigma_{Tg} - \mu_g\sigma_{rg}] \\ \varepsilon_{Tm} = \frac{1}{E_m} [(1 - \mu_m)\sigma_{Tm} - \mu_m\sigma_{rm}] + \beta_m\omega_m \end{cases} \quad (11)$$

According to the deformation coordination condition, it is known that the tangential strains of hollow glass beads as well as epoxy resin at the interface are equal:

$$\varepsilon_{Tg} = \varepsilon_{Tm} \quad (12)$$

Substituting Eq. (11) into Eq. (12) yields:

$$\frac{1}{E_g} [(1 - \mu_g)\sigma_{Tg} - \mu_g\sigma_{rg}] = \frac{1}{E_m} [(1 - \mu_m)\sigma_{Tm} - \mu_m\sigma_{rm}] + \beta_m\omega_m \quad (13)$$

Substituting Eq. (10) into Eq. (13) yields:

$$\frac{1}{E_g} [(1 - \mu_g)G_p\sigma_{ri} + \mu_g\sigma_{ri}] = \frac{1}{E_m} [(1 - \mu_m)M_p\sigma_{ri} + \mu_m\sigma_{ri}] + \beta_m\omega_m \quad (14)$$

Simplifying Eq. (14) yields the interface stress the radial stress at the interface:

$$\sigma_{ri} = \frac{E_m E_g \beta_m \omega_m}{E_m [(1 - \mu_g)G_p + \mu_g] - E_g [(1 - \mu_m)M_p + \mu_m]} \quad (15)$$

Substituting Eq. (15) into Eq. (8) yields the bulk stress of the resin at the microscale:

$$\Theta^{mic} = \frac{3r_i^3}{r_m^3 - r_i^3} \frac{E_m E_g \beta_m \omega_m}{E_m [(1 - \mu_g)G_p + \mu_g] - E_g [(1 - \mu_m)M_p + \mu_m]} \quad (16)$$

2.3. Calculation of the bulk stress at the mesoscale

The distribution of water absorption in the thickness direction is not uniform. This means that the hygroscopic strain in the thickness direction is also not uniform. As shown in Fig. 2, the nonuniform distribution of hygroscopic strain in the thickness direction leads to the generation of internal stress. Since the thickness of the thin plate is on the order of millimetres, we call the stress in this scale *meso* stress. The internal stresses will affect the diffusion coefficient as well as the water absorption behaviour.

The hollow glass bead/resin composite per unit length is selected for analysis. Therefore, the hygroscopic strain $\varepsilon^w(z)$ is the deformation of the hollow glass bead/resin composite due to water absorption, the stress-strain $\varepsilon^\sigma(z)$ is the deformation due to internal stress, and the sum of the two is the total strain $\bar{\varepsilon}$ of the hollow glass bead/resin composite.

The total strain in the x and y directions is equal and constant according to the symmetry. The x and y directions also have equal water absorption distributions. Therefore, the hygroscopic strains are equal. The total strain consists of both stress-induced strain and hygroscopic strain. It can be further deduced that the stress-induced strain and stress distribution in both the x and y directions are also equal. Therefore:

$$\bar{\varepsilon} = \varepsilon^\sigma(z) + \varepsilon^w(z) \quad (17)$$

Applying the formula for linear hygroscopic strain, it follows that:

$$\bar{\varepsilon} = \varepsilon^\sigma(z) + \beta_b\omega(z) \quad (18)$$

where, $\bar{\varepsilon}$ is the total strain in the x or y direction; $\varepsilon^\sigma(z)$ is the strain caused by stress; $\varepsilon^w(z)$ is the strain caused by water absorption. $\omega(z)$ is the hygroscopic rate at z . The relationship between the stress and the strain caused by stress is:

$$\sigma(z) = Q\varepsilon^\sigma(z) \quad (19)$$

where, $\sigma(z)$ is the stress at z and Q is the stiffness matrix of the hollow glass bead/resin composite. Substituting Eq. (18) into Eq. (19) yields:

$$\sigma(z) = Q(\bar{\varepsilon} - \beta_b\omega(z)) \quad (20)$$

When the hollow glass bead/resin composite is considered to be an isotropic material, there are only normal stresses between adjacent interfaces. Both the shear stress and shear strain are zero. Therefore:

$$\sigma(z) = \begin{bmatrix} \sigma(z) \\ \sigma(z) \\ 0 \end{bmatrix}, \quad Q = \begin{bmatrix} \frac{E_b}{1 - \mu_b^2} & \frac{\mu E_b}{1 - \mu_b^2} & 0 \\ \frac{\mu E_b}{1 - \mu_b^2} & \frac{E_b}{1 - \mu_b^2} & 0 \\ 0 & 0 & G_{12} \end{bmatrix} \quad (21)$$

Where, E_b is the elastic modulus of the hollow glass bead/resin composite. In this experiment, the water pressure on the hollow glass bead/resin composite is only about 1000 Pa. It has little influence on the water absorption and stress of the hollow glass bead/resin composite, which can be ignored. According to the stress balance conditions, there is:

$$F = \int_0^h \sigma(z) dz = 0 \quad (22)$$

In this equation, F is the resultant force in the x or y direction. Applying the formula for stress in Eq. (20), the result is:

$$\int_0^h Q(\bar{\varepsilon} - \beta_b\omega(z)) dz = 0 \quad (23)$$

Substituting Eq. (21) into Eq. (23) yields:

$$\frac{E_b}{1 - \mu_b^2} (\bar{\varepsilon}h - \beta_b \int_0^h \omega(z) dz) + \frac{\mu_b E_b}{1 - \mu_b^2} (\bar{\varepsilon}h - \beta_b \int_0^h \omega(z) dz) = 0 \quad (24)$$

Simplifying this formula yields:

$$\bar{\epsilon} = \frac{\beta_b}{h} \int_0^h \omega(z) dz \quad (25)$$

According to the expression of Eq. (25), the total strain of the sheet is the average value of the hygroscopic strain. The water absorption of the sheet is nonuniformly distributed in the thickness direction. The water absorption of the thin sheet is:

$$\bar{\omega} = \frac{1}{h} \int_0^h \omega(z) dz \quad (26)$$

Substituting Eq. (26) into Eq. (27) yields:

$$\bar{\epsilon} = \beta_b \bar{\omega} \quad (27)$$

Substituting Eq. (27) into Eq. (20) yields the stress distribution in the thickness direction:

$$\sigma(z) = Q\beta_b(\bar{\omega} - \omega(z)) \quad (28)$$

The concentric spherical shell model and the spherical shell-cube model have their own advantages and disadvantages, but both can be used as RVEs for hollow glass bead/resin composites. Therefore, the bulk stress of resin in the concentric spherical shell model under uniformly distributed load p is equal to that of resin in the spherical shell-cube model under three-dimensional load p . Then, according to the symmetry, the deformation and bulk stress distribution of the two models are equal. In the reference (Wang and Cui, 2020), the radial stresses at the interface for a concentric spherical-shell model under a uniform load p are given:

$$\sigma_{r_i}^p = -\frac{E_g(1-\mu_m)M_0p}{E_m[(1-\mu_g)G_p + \mu_g] - E_g[(1-\mu_m)M_p + \mu_m]} \quad (29)$$

where $M_0 = 3/2(1-V_g)$. The bulk stress of the resin in the concentric spherical shell model under a uniform load p is:

$$\Theta^{mes} = \sigma_{r_m} + 2\sigma_{T_m} = \frac{3(r_m^3p - r_i^3\sigma_{r_i}^p)}{r_m^3 - r_i^3} \quad (30)$$

Substituting Eq. (29) into Eq. (30) yields:

$$\Theta^{mes} = \frac{3p}{r_m^3 - r_i^3} \left(\frac{r_i^3 E_g (1 - \mu_m) M_0}{E_m [(1 - \mu_g) G_p + \mu_g] - E_g [(1 - \mu_m) M_p + \mu_m]} + r_m^3 \right) \quad (31)$$

This formula is the bulk stress of the matrix under three-dimensional load p . It is equal to the bulk stress of resin in the spherical shell-cube model under three-dimensional load. Therefore, the bulk stress of the spherical shell-cube model under a uniformly distributed load p in the x and y directions (see Fig. 3) should be:

$$\Theta^{mes} = \frac{2p}{r_m^3 - r_i^3} \left(\frac{r_i^3 E_g (1 - \mu_m) M_0}{E_m [(1 - \mu_g) G_p + \mu_g] - E_g [(1 - \mu_m) M_p + \mu_m]} + r_m^3 \right) \quad (32)$$

Assuming there is a very thin layer in the thickness direction of the hollow glass bead/resin composite, the thickness is dh (see Fig. 3). The hygroscopic stresses in the x, y directions are equal to $\sigma(z)$. Then, the bulk stress of the resin in this thin layer is:

$$\Theta^{mes} = \frac{2\sigma(z)}{r_m^3 - r_i^3} \left(\frac{r_i^3 E_g (1 - \mu_m) M_0}{E_m [(1 - \mu_g) G_p + \mu_g] - E_g [(1 - \mu_m) M_p + \mu_m]} + r_m^3 \right) \quad (33)$$

Substituting Eq. (28) into Eq. (33) yields the bulk stress of the resin under mesoscale stress:

$$\Theta^{mes} = \frac{2Q\beta_b(\bar{\omega} - \omega(z))}{r_m^3 - r_i^3} \left(\frac{r_i^3 E_g (1 - \mu_m) M_0}{E_m [(1 - \mu_g) G_p + \mu_g] - E_g [(1 - \mu_m) M_p + \mu_m]} + r_m^3 \right) \quad (34)$$

According to Eq. (1), to obtain the diffusion coefficient under the stress state, the bulk stress of the resin should be calculated first, including both microscale and mesoscale:

$$\Theta^m = \Theta^{mic} + \Theta^{mes} \quad (35)$$

The work of reference (Wang et al., 2017) has proven that the relationship between the diffusion coefficient under a three-dimensional stress state and the initial diffusion coefficient is consistent with Eq. (1):

$$D_\sigma = D_0 \exp\left(\frac{\alpha\Theta^{mic}}{G} + \frac{\alpha\Theta^{mes}}{G}\right) \quad (36)$$

Substituting Eq. (16) and Eq. (34) into Eq. (36) yields the relationship between the diffusion coefficient and stress. Since the model includes the calculation of volume stress at meso- and microscales and describes the coupling relationship between stress and water absorption behaviour, we call it a cross-scale hygro-mechanical coupling model.

2.4. Simplified hygro-mechanical coupling model

According to the Taylor series expansion (Attaway, 2013), if $|x| < 0.1$, there is $e^x \approx 1 + x$. Therefore, if $-0.1 < \alpha\Theta/G < 0.1$, then:

$$D_\sigma(z) = D_0 \exp\left(\frac{\alpha\Theta^m}{G}\right) \approx D_0 \left(1 + \frac{\alpha\Theta^m}{G}\right) = D_0 \left(1 + \frac{\alpha\Theta^{mic}}{G} + \frac{\alpha\Theta^{mes}}{G}\right) \quad (37)$$

In Eq. (16), ω_m is the water absorption at the microscale. Its expression is the ratio of water mass to matrix mass, while $\omega(z)$ in Eq. (34) is the water absorption at the mesoscale. It is the ratio of the mass of water to the mass of hollow glass bead/resin composite, and it is non-uniformly distributed in the thickness direction. ω_m is obviously proportional to $\omega(z)$ (see Table 4). In this equation, all parameters are constant, except ω_m . Considering that in Eq. (16), all parameters except ω_m are constants. Therefore, we can define two proportional constants, k_1 and k_2 :

$$\begin{cases} \frac{\alpha\Theta^{mic}}{G} = k\omega(z) \\ \frac{\alpha\Theta^{mes}}{G} = b(\bar{\omega} - \omega(z)) \end{cases} \quad (38)$$

Substituting Eq. (38) into Eq. (37) yields the relationship between the diffusion coefficient of the hollow glass bead/resin composite and the initial diffusion coefficient under stress:

$$D_\sigma(z) = D_0 [1 + k\omega(z) + b(\bar{\omega} - \omega(z))] \quad (39)$$

where, $D_\sigma(z)$ is the diffusion coefficient of a point in the thickness direction.

In deriving Fick's second law, it is assumed that the diffusion coefficient does not vary with space. However, the nonuniform distribution of hygroscopic stress determines that the diffusion coefficient varies in the thickness direction. This requires the calculation of the equivalent diffusion coefficient of the hollow glass bead/resin composite. In this paper, the average value of the diffusion coefficient of each layer was taken as the equivalent diffusion coefficient of the composite material:

$$\begin{aligned} \bar{D}_\sigma &= \frac{1}{h} \int_0^h D_0 [1 + k\omega(z) + b(\bar{\omega} - \omega(z))] dz \\ &= D_0 \left[1 + \frac{k}{h} \int_0^h \omega(z) dz + b \left(\bar{\omega} - \frac{1}{h} \int_0^h \omega(z) dz \right) \right] \end{aligned} \quad (40)$$

Table 1
The particle distribution of K1.

Proportion (%)	10	50	90	Max
Particle (μm)	30	65	110	120

Table 2
The material parameters of matrix, glass and K1.

Objects	E (GPa)	μ	ρ (g/cm ³)	β	C_m (%)
E51	2.10	0.30	1.100	0.52	2.50
Glass	60.00	0.23	2.180	0.00	0.00
K1		\	0.125	0.00	0.00

Table 3
The material parameters of hollow glass bead/resin composite materials.

Specimens	V_g (%)	r_m (μm)	ρ (g/cm ³)	E_b (GPa)	μ_b	β_b
B-1	30	48.55	0.81	1.90	0.30	0.57
B-2	40	44.11	0.71	1.80	0.29	0.53
B-3	50	40.95	0.61	1.75	0.28	0.48
B-4	60	38.53	0.52	1.70	0.28	0.41

Table 4
Diffusion coefficient and saturated water absorption of the specimens.

Specimens	$\omega_m / \omega(z)$	C_m (%)	D_0 ($\times 10^{-7}$ mm ² /s)
B-1	1.05	1.70	12.32
B-2	1.08	1.60	8.50
B-3	1.11	1.51	7.42
B-4	1.18	1.46	6.31

Substituting Eq. (26) into Eq. (40) yields a simplified model of the diffusion coefficient for the hollow glass bead/resin composite after water absorption without considering the water pressure:

$$\bar{D}_e = D_0(1 + k\bar{\omega}) \quad (41)$$

Eq. (41) is the simplified hygro-mechanical coupling model for the hollow glass bead/resin composites. Obviously, this simplified model only needs to measure the water absorption of the hollow glass bead/resin composite samples and calculate k according to the experimental data to obtain the relationship between the diffusion coefficient and water absorption. This means that the simplified model is more suitable for engineering applications. However, the effectiveness of this simplified model needs to be verified by both original model and the experimental results. The effective water absorption range of the simplified model will be studied in subsequent work.

3. Experiments

3.1. Test subjects

This subsection will refer to the specification ASTM D5229 (2010) for the water absorption test of hollow glass bead/resin composites. Then, their saturation absorption and diffusion coefficients were calculated according to the experimental data. The hollow glass bead/resin composite was prepared by CSSC 725 research institute in China. The hollow glass beads are K1 produced by 3 M. The epoxy resin is E51. The specimens were divided into 4 groups of 6 each, totaling 24. The numbers are B-1 ~ B-4, and the volume fractions of the corresponding hollow glass beads are 30 %, 40 %, 50 % and 60 % respectively. The specimen size was 60 mm × 60 mm × 2 mm. The particle size distribution of hollow glass beads provided by 3 M is shown in Table 1. The material parameters of epoxy resin, hollow glass beads and glass for preparing hollow glass beads are shown in Table 2. The material parameters of the prepared hollow glass bead/resin composites are shown in Table 3. The data in Table 2 and Table 3 are provided by CSSC 725 research institute.

3.2. Water absorption test method

1) A specimen with uniform thickness and good quality was selected for the test. The specimen was baked in a vacuum oven at 70 °C for 7 h, and then the mass of the specimen was determined using a balance with a 0.1 mg accuracy. The baking-weighing process was repeated until the mass reduction of the specimens was <0.1 mg. At this time, the water content of the specimen can be considered to be approximately 0, and the dried mass is recorded as W_d .

2) The specimens were placed into a stainless steel cage containing a certain counterweight. As shown in Fig. 4, the erected stainless steel block is used as a counterweight to completely immerse the metal cage and sample in water. At the same time, separate the sample and keep standing to ensure that moisture diffusion occurs on both sides of the sample. The metal cage containing the specimen was immersed in distilled water at room temperature (23 ± 2 °C) for a certain time. Then, the specimen was removed, wiped dry with absorbent paper and weighed. The mass of the specimen is written as W_w . The hydroscopic rate of the specimen at this moment is:

$$M_t = \frac{W_w - W_d}{W_d} \times 100\% \quad (42)$$

where M_t is the hydroscopic rate of the composite laminate at time t .

3) After testing the water absorption mass of the specimen, the specimen was placed in distilled water again. After soaking for a certain time, the sample mass was determined. The entire process was completed within 15 min. When the difference between the hydroscopic

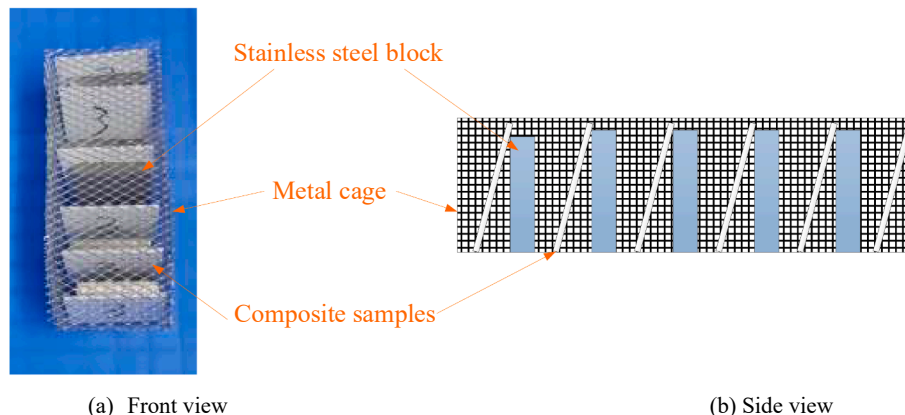


Fig. 4. Water absorption test method.

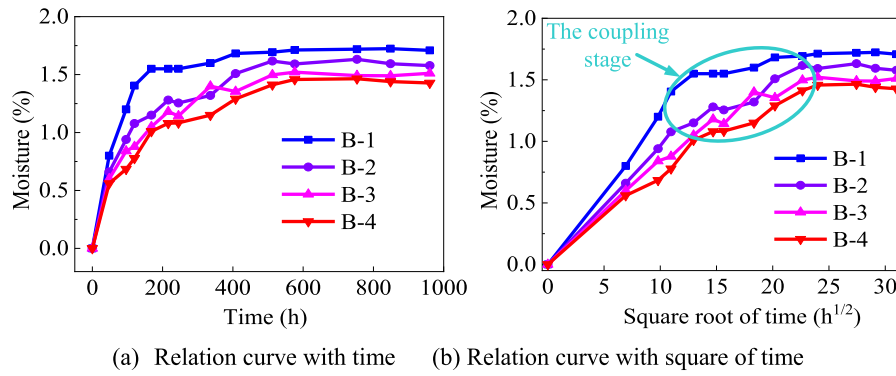


Fig. 5. The relation curve of water absorption.

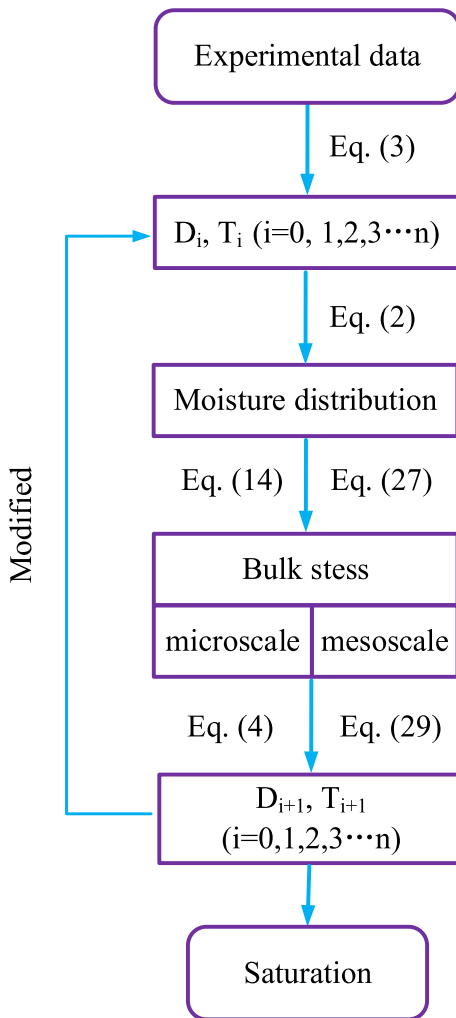


Fig. 6. The moisture diffusion coupled with stress calculation process for the hollow glass bead/resin composite materials.

rate measured more than 5 times in a row does not exceed 5 % and the hydroscopic rate no longer increases, the specimen can be considered to have reached saturation. Then, the test was stopped.

3.3. Test results

The mass of the hollow glass bead/resin composite specimens was recorded at different times, and the hydroscopic rate was calculated, as

shown in Fig. 5(a). The relationship curve between hydroscopic rate and square root of time is shown in Fig. 5(b). It shows there is a nonlinear stage of water absorption. The results of each group were averaged to calculate the average hydroscopic rate and record the measurement time. The diffusion coefficient and the saturation hydroscopic rate were obtained according to Eq. (3), as shown in Table 4. What worth noting is that the diffusion coefficient measured in the experiment is not a parameter in ideal state, but parameters including the effects of porosity, impurities, interfaces and others. Therefore, the impacts of these factors are not necessarily considered in the calculation process.

4. Analysis

4.1. Calculation process of the coupling model

The calculation process of the hygro-mechanical coupling model is shown in Fig. 6. The specific calculation process is as follows:

1) The diffusion coefficient and saturation hydroscopic rate of the hollow glass bead/resin composite specimen are obtained by combining the experimental data with Eq. (3) (see Table 4). Then, the hydroscopic rate distribution in the thickness direction of the hollow glass bead/resin composite is calculated according to Eq. (5).

2) Based on the theoretical model, the bulk stress of the polymer matrix at the microscopic and mesoscale scales is calculated. Then, the distribution of the diffusion coefficients in the thickness direction according to the diffusion coefficient model in the three-dimensional stress state is calculated. The diffusion coefficients in the thickness direction are averaged as the diffusion coefficient of the whole hollow glass bead/resin composite sheet in the second time period. The equivalent diffusion time of the second time period is calculated according to the equivalent diffusion time model.

3) Finally, the diffusion coefficient and the equivalent diffusion time of the entire sheet in the second time period are substituted into Eq. (5) to calculate the hydroscopic rate distribution in the thickness direction in the second time period. This cycle is repeated until the hollow glass bead/resin composite reaches saturation. If $t_1 = 0, C_1 = 0$, according to prediction, the results without considering the hygro-mechanical coupling can be calculated by Eq. (3):

$$D_0 = \pi \left(\frac{h}{4C_m} \right)^2 \frac{C(t)}{t} \tag{43}$$

$$\Rightarrow C(t) = \frac{4C_m}{h} \sqrt{\frac{D_0 t}{\pi}}$$

The comparisons among prediction results of coupling model, simplified model, the model without coupling and the experimental data are shown in Fig. 7. It is showed that the comparison results of the coupled model and the simplified model are in great consensus. However, the model without considering the hygro-mechanical coupling cannot accurately predict the water absorption after 100 h. This displays

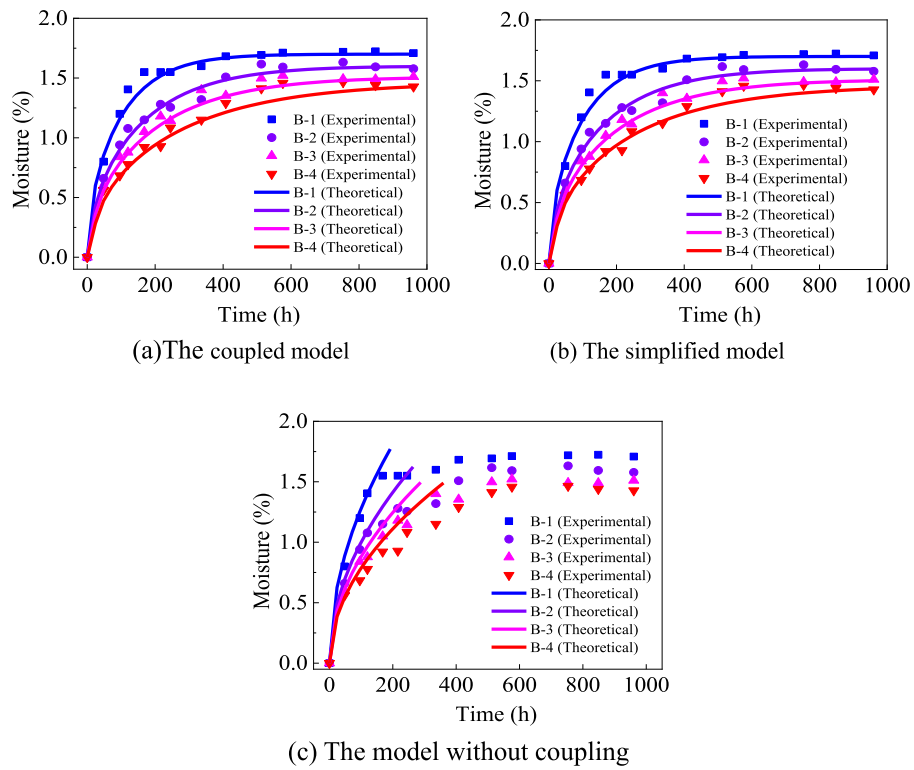


Fig. 7. The prediction results of the coupled model, the simplified model and the model without coupling.

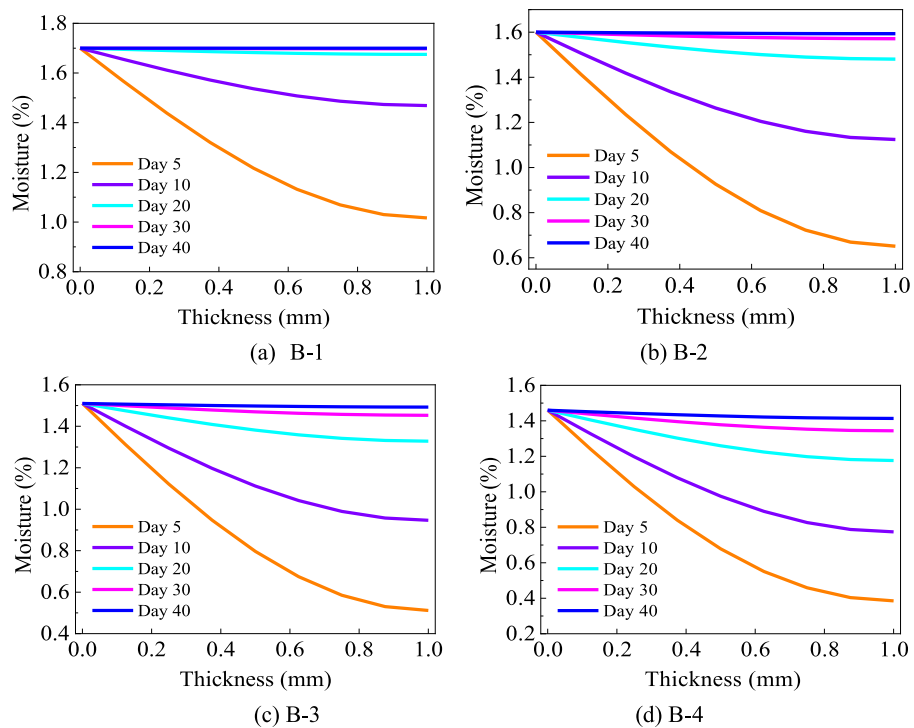


Fig. 8. The distribution of water absorption in the thickness direction of the sample at different times.

that it is necessary to consider the effects of the hygro-mechanical coupling.

4.2. Variation laws in water absorption

Fig. 7 shows that the prediction results of the simplified model are

basically the same as those of the coupled model. There, only the prediction results of the coupled model will be used in subsequent work. The distribution of water absorption in the thickness direction of the hollow glass bead/resin composite at days 5, 10, 20, 30, and 40 was calculated as shown in Fig. 8. Considering the symmetry of the water absorption in the thickness direction of the sheet, only the water

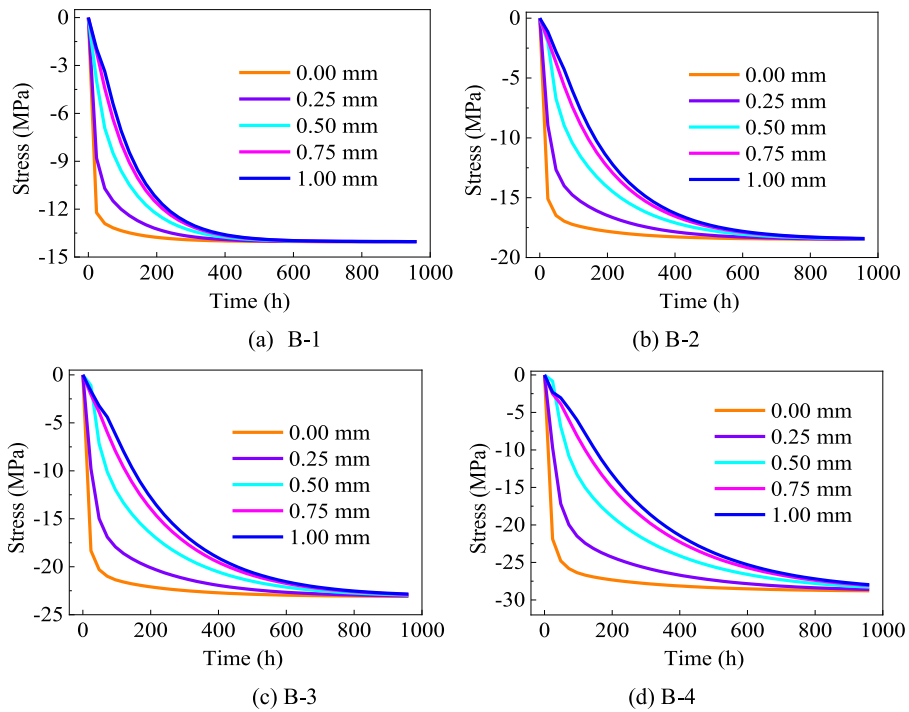


Fig. 9. The variation curve of micro bulk stress at different positions in thickness direction.

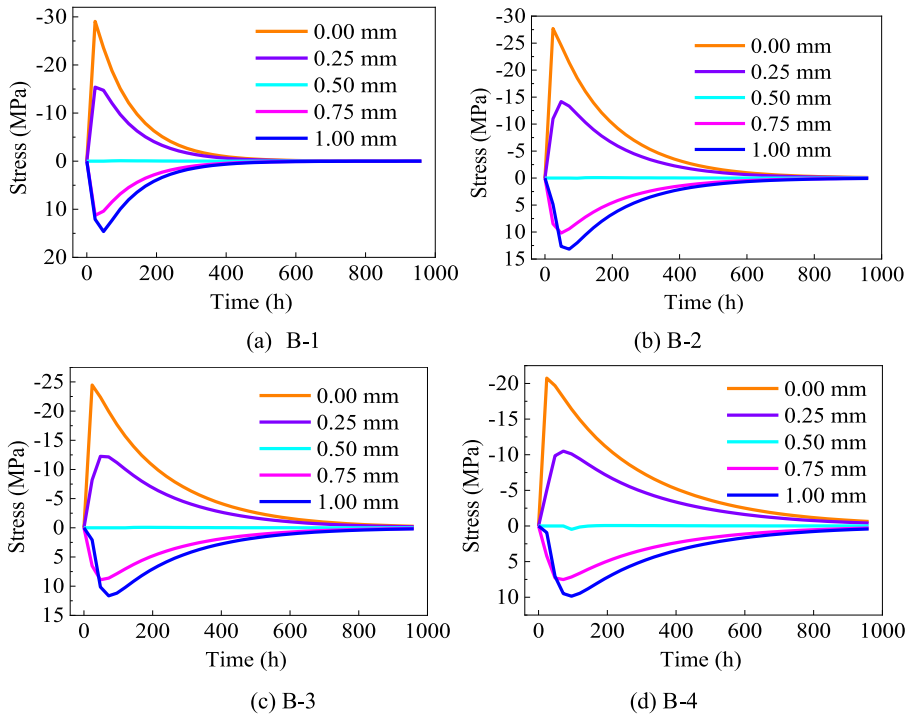


Fig. 10. The variation curve of meso bulk stress at different positions in thickness direction.

absorption distribution of half of the thickness is given here. It can be seen that the hygroscopic rate on the surface of the hollow glass bead/resin composite reaches saturation in a short time and no longer changes. The hygroscopic rate in the middle position of the thin plate is the lowest and gradually increases with time until it reaches saturation. Comparing B-1 to B-4, it can be seen that the hygroscopic rate of the hollow glass bead/resin composite decreases with increasing volume fraction of hollow glass beads. The reason is that the increase of volume

fraction of hollow glass beads hinders the diffusion of water molecules in the hollow glass bead/resin composite.

Considering the symmetry of the stress distribution in the thickness direction, the surface (0.0 mm), 0.5 mm and 1.0 mm of the hollow glass bead/resin composite sheet are selected as reference points. The microscopic and mesoscale bulk stresses at the reference points are given in Fig. 9 and Fig. 10 respectively. Fig. 9 shows that the microscopic-scale bulk stresses of the hollow glass bead/resin composite

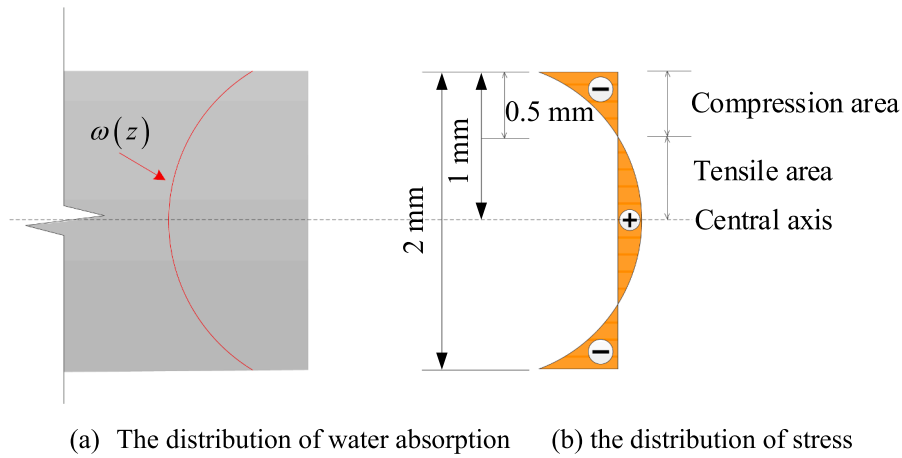


Fig. 11. The stress compression area and tension area in thickness direction.

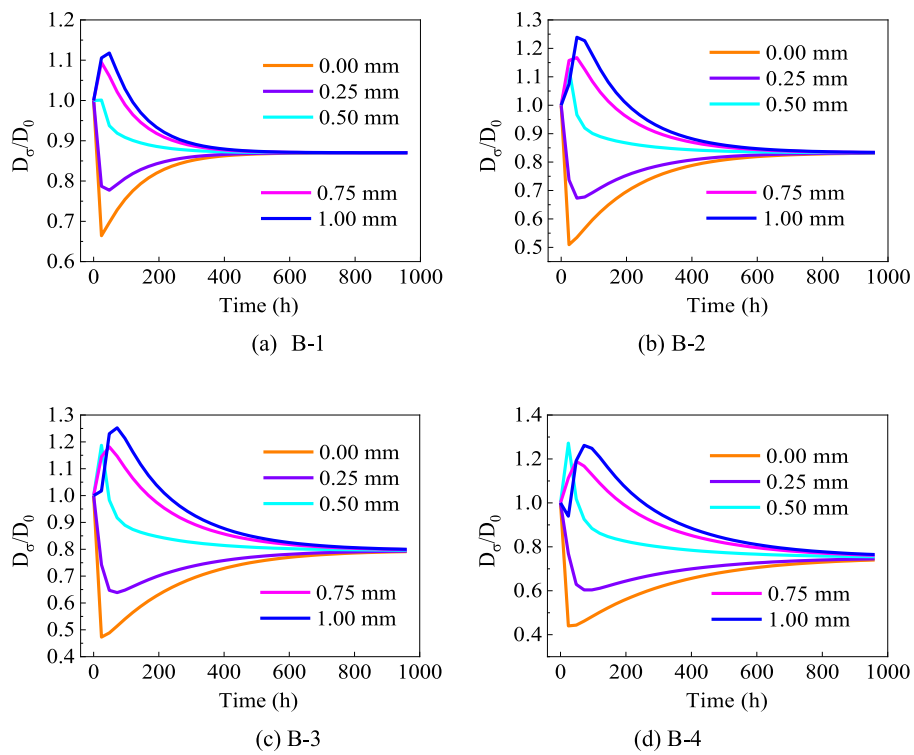


Fig. 12. The variation curve of diffusion coefficient at different positions in thickness direction.

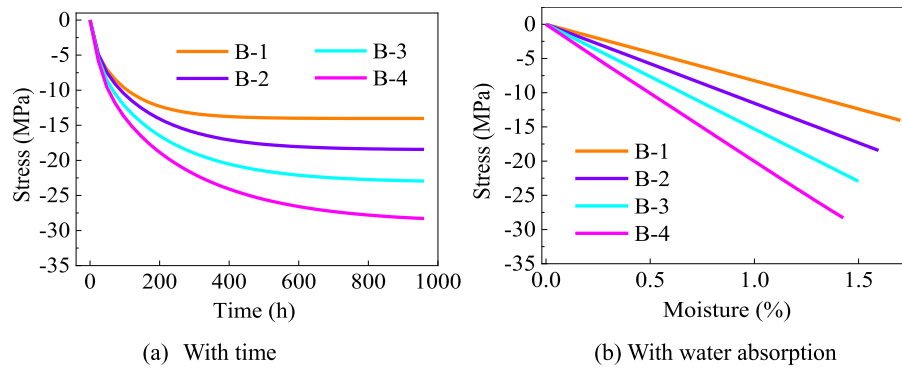


Fig. 13. The curves of bulk stress versus with time and water absorption.

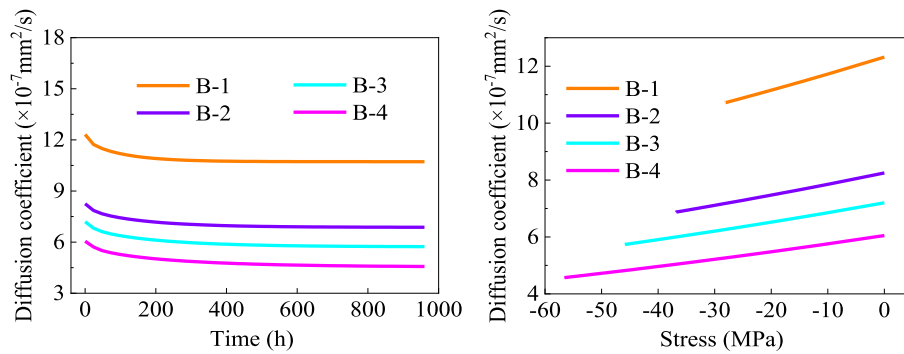


Fig. 14. The relation curve of diffusion coefficient with time and bulk stress.

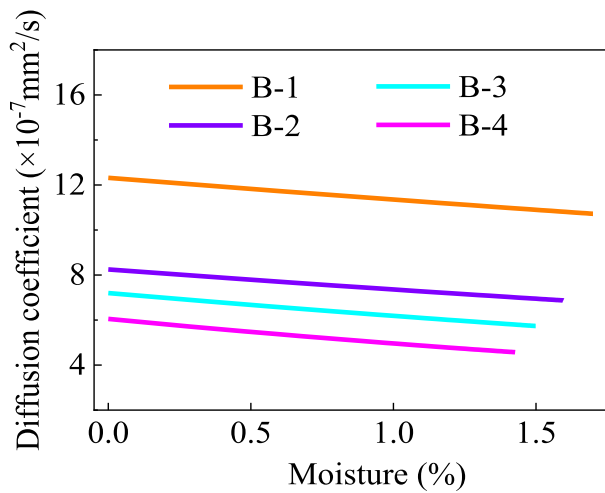


Fig. 15. The linear relationship between diffusion coefficient and water absorption.

exhibit compressive stresses after water absorption. Comparing the microscale bulk stresses at different locations, it can be seen that the microscale bulk stresses at the surface are the largest and the smallest at the middle thickness. Comparing B-1 to B-4, it can be seen that the microscale bulk stress increases with increasing volume fraction of hollow glass beads. This is because the increase in the volume fraction of hollow glass beads increases the interaction between the resin matrix and hollow glass beads.

The distribution of bulk stresses at the mesoscale in the thickness direction is also symmetric. Fig. 10 shows that the bulk stress at the mesoscale is divided at 0.5 mm. The stress in the range of 0 ~ 0.5 mm is compressive stress, while the stress in the range of 0.5 ~ 1.0 mm is tensile stress (see Fig. 11). This is caused by the mismatch between the hygroscopic strain in the compression area and the tension area. From the curve of bulk stress versus time, the mesoscale bulk stress will first increase with increasing water absorption. After reaching a peak gradually, the mesoscale bulk stress decreases because the increase in water absorption in the tension area causes a decrease in its restraint capacity on the compression area. Comparing B-1 to B-4, it can be seen that with the increase in the volume fraction of hollow glass beads, the mesoscale bulk stress decreases. This is because the increase in the volume fraction of hollow glass beads reduces the water absorption of the hollow glass bead/resin composite sheet, which leads to a decrease in the stress in the thickness direction.

The variation curve of the diffusion coefficient at the reference point with time is given in Fig. 12. The diffusion coefficient generally decreases with time, which is very similar to the curve of the bulk stress at the mesoscale. This indicates that the distribution of the diffusion

Table 5

Proportional constants for the specimens.

Specimens	m	$n (\times 10^{-9})$	k
B-1	-8.256	5.65	-7.61
B-2	-11.550	3.78	-10.62
B-3	-15.304	3.24	-13.84
B-4	-19.964	2.68	-17.72

coefficient is more influenced by the bulk stress at the mesoscale. There is an increase in the diffusion coefficient in the range of 0.50 ~ 1.00 mm of the hollow glass bead/resin composite plates. It is even larger than the initial diffusion coefficient because it is subjected to tensile stresses, which can increase the free volume fraction of the matrix.

The curves of bulk stress versus time and water absorption for the entire thin plate of the hollow glass bead/resin composite are given in Fig. 13. The bulk stress increases gradually with time and linearly with the hygroscopic rate. Comparing B-1 to B-4, it can be seen that with the increase in the volume fraction of hollow glass beads, the bulk stress of the entire thin plate gradually increases. This is similar to the trend of microscopic bulk stress, and it is not difficult to determine that the microscopic bulk stress plays the dominant role.

The diffusion coefficient versus time as well as the bulk stress curve is given in Fig. 14. The diffusion coefficient of the entire thin plate gradually decreases with time because the compressive stress generated by the water absorption of the hollow glass bead/resin composite leads to a reduction in the free volume fraction of the resin matrix. The diffusion coefficient of the entire thin plate decreases linearly with the bulk stress because $-0.1 < \alpha\theta/G < 0.1$. In this range, the exponential function can be approximated to be linear.

According to Fig. 14, it is not difficult to infer that the diffusion coefficient of the entire thin plate is approximately linear with the hygroscopic rate, as shown in Fig. 15. Table 5 calculates the proportionality constants of bulk stress vs water absorption, diffusion coefficient vs bulk stress, and diffusion coefficient vs water absorption. The negative value of the proportionality constant k indicates that the diffusion coefficient decreases with increasing water absorption. Comparing B-1 to B-4, it can be seen that the slope k increases with the increase in the volume fraction of hollow glass beads. The reason is that the bulk stress of the entire sheet increases with increasing volume fraction of hollow glass beads (see Fig. 13). This makes the change rate of the diffusion coefficient increase. Therefore, the slope is also large.

The simplified model can only hold for a certain range. If we can give a range of water absorption in which the simplified model is effective, this range would be very useful for engineering applications. Fig. 15 shows the comparison between the diffusion coefficients predicted by the simplified model and the diffusion coefficients predicted by the hygro-mechanical coupling model at a hygroscopic rate of 0 ~ 5 % for B-1 ~ B-4. The curves of deviation versus time in this range are also given. The deviation increases with increasing hygroscopic rate. Taking B-4,

which has the largest deviation, as an example, when the hygroscopic rate is 2.0 %, the deviation between the simplified model and the hygro-mechanical coupling model prediction is 4.0 %. At this time, the deviation is acceptable, and the simplified model is valid. The saturated water absorption of specimens B-1 to B-4 is also exactly in this range.

5. Conclusions

In this paper, a hygro-mechanical coupling model of hollow glass bead/resin composites is established based on classical mechanics analysis. The validity of the model is verified through comparison with the experimental results. The evolution law of the hygroscopic rate, stress distribution and diffusion coefficient of the hollow glass bead/resin composite after water absorption was analyzed based on this model.

The distribution and variation of stress, hygroscopic rate and diffusion coefficient, as well as the law of increasing with the volume fraction of hollow glass beads were studied. The diffusion coefficients predicted by the simplified model and the diffusion coefficients predicted by the hygro-mechanical coupling model at a hygroscopic rate of 0 ~ 5 % are compared. The curves of deviation versus time in this range are also given. The deviation increases with increasing hygroscopic rate. It was determined by calculation that when the hygroscopic rate is 2.0 %, the

deviation between the simplified model and the hygro-mechanical coupling model prediction is <4.0 %. At this time, the deviation is acceptable, and the simplified model is valid. The saturated water absorption of all the specimens in this paper is also in this range.

Declaration of Competing Interest

The authors declare that they have no known competing financial interests or personal relationships that could have appeared to influence the work reported in this paper.

Data availability

No data was used for the research described in the article.

Acknowledgements

This work is supported by the General Program of National Natural Science Foundation of China ‘Study on water absorption characteristics of buoyancy material in full ocean depth manned submersible’ (Grant No.51879157), the National Natural Science Foundation of China for Youth Science Project ‘Mechanism of stress-moisture-creep coupling on compressive strength of composites in deep-sea’ (Grant No.11902288).

Appendix

List of variables

D_m, D_0	the diffusion coefficients of the matrix in the stressed and free states
G_m	the shear modulus of the matrix
C_m	the saturated water absorption of the composite laminate
h	the thickness of the composite laminate
t	the time parameter
μ_m, μ_g	Poisson’s ratios of the matrix and glass
σ_r	the radial stress at the interface between the glass bead and the matrix
$\sigma_{r_g}, \sigma_{T_g}$	the radial and circumferential normal stresses in glass shell
$\sigma_{r_m}, \sigma_{T_m}$	the radial and circumferential normal stresses in the matrix shell
$\Theta^{mic}, \Theta^{mes}$	the volume stresses at microscopic and mesoscopic scales
E_m, E_g	the elastic modulus of the matrix and glass
β_m, β_b	the hygroscopic coefficients of the matrix and
ω_m	the water absorption of the matrix and the composite

References

Apicella, A., Nicolais, L., 1985. In: Effect of water on the properties of epoxy matrix and composites. Springer, Berlin Heidelberg, pp. 69–77.

ASTM D5229. Standard test methods for moisture absorption properties and equilibrium conditioning of polymer matrix composite materials. In Annual Book of Standards. 2010.

Attaway S. Advanced Mathematics. Matlab (Third Edition), A Practical Introduction to Programming and Problem Solving. 2013.

Boukert B, Benkhedda A, B Adda E, Khodjet-Kesba M. Hygrothermal Stresses Analysis of Thick Composite Plates Using High Order Theory Under a Fick Concentration Distribution. Procedia Structural Integrity. 2019, 17: 37-43.

Carter, H.G., Kibler, K.G., 1978. Langmuir-Type Model for Anomalous Moisture Diffusion In Composite Resins. J. Compos. Mater. 12 (2), 118–131.

Catalanotti, G., Sebaey, T.A., 2019. An algorithm for the generation of three-dimensional statistically Representative Volume Elements of unidirectional fibre-reinforced plastics: Focusing on the fibres waviness. Compos. Struct. 227, 111272.

Corigliano, A., Rizzi, E., Papa, E., 2000. Experimental characterization and numerical simulations of a syntactic-foam/glass-fibre composite sandwich. Compos. Sci. Technol. 60, 2169–2180.

David A, Biro. Gerald Pleizier, Yves Deslandes. Application of the Microbond Technique: Effects of Hygrothermal Exposure on Carbon-Fiber/Epoxy Interfaces. Composites Science and Technology. 1993, 46(3): 293–301.

Ghorbed I, valentin D. Hygrothermal Effects on the Physico-Chemical Properties of Pure and Glass-Fiber Reinforced Polyester and Vinylester Resins. Polymer Composites. 1993, 14 (4): 324–334.

Gueribiz, D., Jacquemin, F., Fréour, S., 2013. A moisture diffusion coupled model for composite materials. Eur. J. Mech. A/Solids. 42, 81–89.

Guo, R., Xian, G.J., Li, C.G., Hong, B., Huang, X.Y., Xin, M.Y., Huang, S.D., 2021. Water uptake and interfacial shear strength of carbon/glass fiber hybrid composite rods under hygrothermal environments: effects of hybrid modes. Polym. Degrad. Stab. 193, 109723.

Hou, J.Y., Shi, Y.T., Li, Z.H., Wu, J.Q., Gong, J.Y., Zou, W.F., Zuo, H., Ning, D.Y., 2020. Numerical simulation and experimental study on flexible buoyancy material of hollow glass microsphere and silicone rubber for small deep-sea soft robots. Appl. Mater. Today 21, 100875.

Ishai, O., 1975. Environmental Effects of Deformation, Strength and Degradaion of Unidirectional Glass-Fiber Reinforced Plastics. Polym. Eng. Sci. 15 (1), 486–490.

Kumosa, L., Benedikt, B., Armentrout, D., Kumosa, M., 2004. Moisture absorption properties of unidirectional glass/polymer composites used in composite (non-ceramic) insulators. Compos. A Appl. Sci. Manuf. 35, 1049–1063.

Le Gall, M., Choqueuse, M., Gac, P.Y., Davies, P., Perreux, D., 2014. Novel mechanical characterization method for deep sea buoyancy material under hydrostatic pressure. Polym. Test. 39, 36–44.

Lee, M.C., Peppas, N.A., 1993. Water Transport in Graphite/ Epoxy Composites. J. Appl. Polym. Sci. 47, 1349–1359.

Meng, M., Rizvi, M.J., Le, H.R., Grove, S.M., 2016. Multi-scale modelling of moisture diffusion coupled with stress distribution in CFRP laminated composites. Compos. Struct. 138, 295–304.

Neumann, S., Marom, G., 1985. Stress dependence of the coefficient of moisture diffusion in composite materials. Polym. Compos. 6 (1), 9–12.

Niu, Y., Wang, S., Zhu, Z.Q., Su, M., Wang, Y.J., Yan, L.J., Ma, Y.J., Sun, H.X., Liang, W. D., Li, A., 2022. Robust composite aerogels with excellent flame retardant and

- thermal insulation properties based on modified hollow glass microspheres. *Polym. Degrad. Stab.* 202, 110030.
- Obeid, H., Clément, A., Fréour, S., Jacquemin, F., Casari, P., 2018. On the identification of the coefficient of moisture expansion of polyamide-6: Accounting differential swelling strains and plasticization. *Mech. Mater.* 118, 1–10.
- Peret, T., Clement, A., Freour, S., Jacquemin, F., 2017. Effect of mechanical states on water diffusion based on the free volume theory: Numerical study of polymers and laminates used in marine application. *Compos. B Eng.* 118, 54–66.
- Peret, T., Clement, A., Freour, S., Jacquemin, F., 2019. Homogenization of Fickian and non-Fickian water diffusion in composites reinforced by hydrophobic long fibers: Application to the determination of transverse diffusivity. *Compos. Struct.* 226 (15), 111191.
- Ren S, Hu XX, Ren HT, Wang MC, Guo AR, Liu JC, HY, Xian L. Development of a buoyancy material of hollow glass microspheres/SiO₂ for high-temperature application. *Journal of Alloys and Compounds.* 2017, 721: 213-219.
- Roy, S., Xu, W.X., Park, S.J., et al., 2000. Anomalous Moisture Diffusion in Viscoelastic Polymers: Modeling and Testing. *J. Appl. Mech.* 67 (2), 391–396.
- Sadd, M., 2009. *Elasticity: Theory, Applications, and Numerics.* Elsevier.
- Selzer, R., Friedrich, K., 1997a. Mechanical properties and failure behaviour of carbon fibre-reinforced polymer composites under the influence of moisture. *Compos. A Appl. Sci. Manuf.* 28 (6), 595–604.
- Selzer, S., Friedrich, K., 1997b. Mechanical Properties and Fatigue Behaviour of Carbon Fiber Reinforced Polymer Composites under the Influence of Moisture. *Composites* 28 A(6), 595–604.
- Shen, C.H., Springer, G.S., 1976. Moisture Absorption and Desorption of Composite Materials. *J. Compos. Mater.* 10 (1), 2–20.
- Wang, J.Z., Cui, W.C., 2020. A Water Absorption Model Based on Self-Consistent Theory for Solid Buoyancy Materials. *Eng Technol Open Acc.* 3 (4), 555620.
- Wang, J.Z., Cui, W.C., Nartey, M.A., Dai, F.H., Peng, H.X., 2022. A virtual scale approach to multi-scale calculations and its application in fiber reinforced composites. *Mech. Mater.* 165, 104184.
- Wang, J.Z., Cui, W.C., 2022. Simplified hygromechanical coupling model and numerical simulation analysis of fibre reinforced composite deep-sea and underwater structures. *Compos. Struct.* 218, 115006.
- Wang, J.Z., Dai, F.H., Ma, L., 2017. A Multi-Scale Moisture Diffusion Coupled with Stress Model for Composite Materials. *Compos. Struct.* 171, 345–359.
- Zhong, Y., Zhou, J.R., 1999. Study of Thermal and Hygrothermal Behaviour of Glass/Vinyl Ester Composites. *J. Reinforced Plast. Compos.* 18 (17), 1619–1629.